

# Influence of self-affine roughness on the friction coefficient of rubber at high sliding velocity

G. Palasantzas\*

Department of Applied Physics, Materials Science Centre, University of Groningen Nijenborgh 4, 9747 AG Groningen, The Netherlands

(Received 26 February 2004; published 10 November 2004)

In this work we investigate the influence of self-affine roughness on the friction coefficient of a rubber body onto a solid surface at high speeds. The roughness is characterized by the rms amplitude  $w$ , the correlation length  $\xi$ , and the roughness exponent  $H$ . It is shown that the friction coefficient decreases with increasing correlation length  $\xi$  and increasing roughness exponent  $H$  for sufficiently large correlation lengths. However, for small correlation lengths the opposite behavior takes place because the system is within the strong roughness limit or equivalently average local surface slopes larger than 1. Moreover, direct plots of the friction coefficient as a function of the roughness exponent  $H$  indicate that as the correlation length  $\xi$  decreases, a maximum of the friction coefficient develops. The latter is followed by a continuous increment of the friction coefficient with increasing  $H$  and decreasing  $\xi$ .

DOI: 10.1103/PhysRevB.70.195409

PACS number(s): 46.55.+d, 62.40.+i, 62.20.Qp, 68.55.Jk

## I. INTRODUCTION

The friction properties associated with a rubber body sliding onto a hard solid surface are important from the fundamental and technological point of view. The latter includes the car industry (e.g., tire construction, wiper rubber blades), cosmetic industry etc.<sup>1-4</sup> The low elastic modulus of rubbers and the high internal friction over a wide range of frequencies makes them different from other solids.<sup>2,5</sup> Sliding, however, onto real solid surfaces occurs predominantly on rough surfaces with some or even significant degrees of randomness.<sup>6,7</sup> In this case, the surfaces usually possess roughness over various length scales rather than a single one, which has to be taken carefully into account in contact-related phenomena as that of adhesion and friction.<sup>5</sup>

The friction force between a rubber body and a hard rough solid substrate has two major contributions that are called hysteric and adhesive.<sup>1</sup> In general, adhesion is the result of molecular bonding between the two surfaces in contact. If the bond strength is the same at all bond sites, the friction force that resists sliding will be proportional to the total area of contact. The adhesive component is important for clean and relative smooth surfaces,<sup>5</sup> which will not be the case here. The hysteric component arise from the oscillating forces that the surface asperities exert onto the rubber surface, leading effectively to cyclic deformations and energy dissipation due to internal frictional damping.<sup>5</sup> As a result the hysteric contribution will have the same temperature dependence as that of an elastic complex modulus  $E(\omega)$  (Ref. 5). In addition, depending on the sliding velocity, the low elastic modulus of rubbers leads to instabilities (that produce detachment waves) at high sliding velocities and relatively smooth surfaces (*Schallamach* waves<sup>1</sup>). This case will be excluded here.

In general, if rubber body slides with velocity  $V$  over a sinusoidal rough surface with period  $L$ , then it will feel fluctuating forces with frequencies  $\omega \approx V/L$ . The contribution of surface roughness to the friction coefficient  $\mu_f$  at a length scale  $L$  is maximum for the frequency  $\omega \approx V/L$ , which is located in the transition regime between rubber (low  $\omega$ )

and glass (high  $\omega$ ) behavior [Fig. 1(a)].<sup>5</sup> Therefore for a random surface with a wide distribution of length scales  $L$ , it will be present a wide distribution of frequency components in the Fourier decomposition of the surface stresses acting on the sliding rubber.<sup>5</sup>

Figure 1(a) shows the general velocity dependence of the rubber coefficient of kinetic friction.<sup>5</sup> After the glassy region for high velocities,  $\mu_f$  saturates to a constant value when wear and local heating effects are ignored.<sup>5</sup> Indeed, it was found that the friction coefficient  $\mu_f$  to scale as  $\mu_f \sim w/\xi^H$  (Ref. 5) with  $w$  the rms roughness amplitude and  $\xi$  the in-plane roughness correlation length. The latter expression indicates that the friction coefficient  $\mu_f$  decreases with increasing roughness exponent  $H$ , and/or increasing correlation length  $\xi$  (assuming fixed rms roughness amplitude  $w$ ).

The result of Persson<sup>5</sup> at high sliding velocities was derived by means of a power-law approximation for the self-affine roughness spectrum, which is valid for lateral wavelengths  $q\xi > 1$  with  $\xi$  the in-plane roughness correlation length. On the other hand, the present work concentrates on the effect of roughness including contributions from roughness wavelengths  $q\xi \leq 1$ , and performing more accurate calculations of the friction coefficient  $\mu_f$  in order to account for more details as a function of the self-affine roughness parameters  $w$ ,  $\xi$ , and  $H$ . The latter will be possible in terms of analytic forms for the roughness spectrum in Fourier space that facilitate exact calculation also of the local surface slope, which is an essential quantity in the theory proposed by Persson to describe rubber friction on rough surfaces.<sup>5</sup>

## II. THEORY OF FRICTION AT HIGH SLIDING VELOCITY

For a rubber body of Young modulus  $E$  and Poisson ratio  $\nu$  that slides on a rough solid surface with velocity  $V$ , the frictional shear stress along the sliding axis [e.g., the  $x$  axis, Fig. 1(b)] is given by<sup>5</sup>

$$\sigma_f = -j \int q_x C(q) P(q) [M_{zz}(-\vec{q}, -q_x V)]^{-1} d^2 \vec{q}. \quad (1)$$

$C(q)$  is the Fourier transform of the autocorrelation function  $C(n) = \langle h(\vec{r})h(0) \rangle$  with  $h(\vec{r})$  the surface roughness height

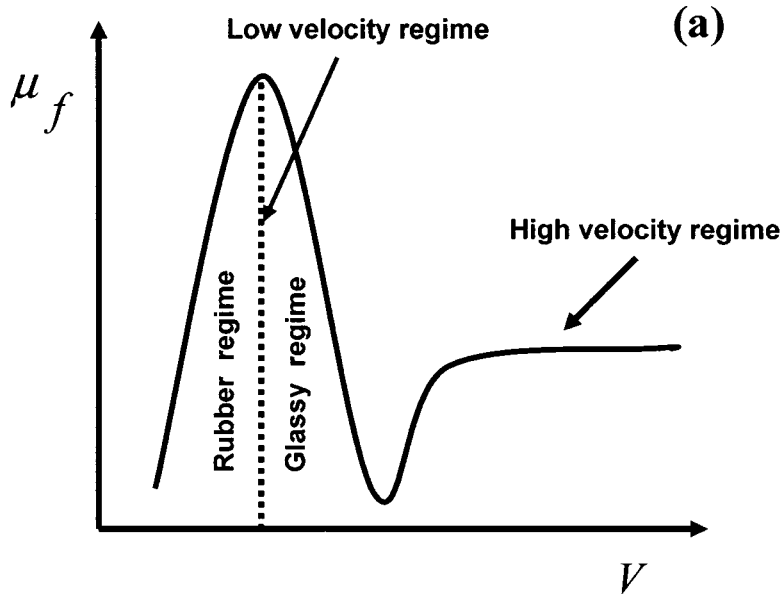
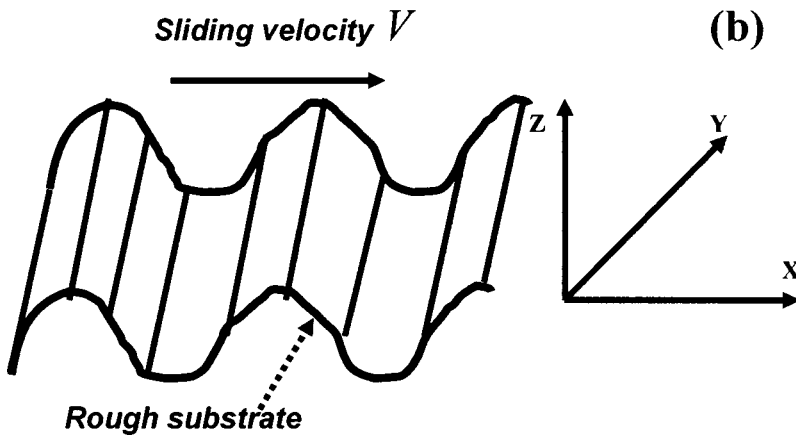


FIG. 1. (a) Schematic of the kinetic friction coefficient of a rubber body sliding onto a rough solid substrate in the absence of local heating and wear effects. (b) Sliding geometry of a rubber body onto a rough solid substrate.



( $\langle h \rangle = 0$ ).  $\langle \dots \rangle$  is an ensemble average over possible roughness configurations.  $M_{zz}$  is the  $z$  component of the tensor that relates the surface stress along the  $z$  direction with the corresponding displacement assumed equal to  $h(\vec{r})$  (Ref. 5). The contact factor  $P(q)$  is the fraction of the original nominal contact area where contact remains when we study the contact area on the length scale  $2\pi/q$  (Ref. 5).

For high sliding velocity or  $V \gg c_L$ , where  $c_L$  is the longitudinal sound velocity in the solid,  $M_{zz}$  is given by (see also the Appendix)<sup>5</sup>

$$M_{zz} = -j(\rho c_L V q_x)^{-1} \quad (2)$$

with  $q_x = q \cos \varphi$  and  $\varphi$  the axis between sliding  $x$  axis and wave vector  $\vec{q} = (q_x, q_y)$  on the  $xy$  plane.  $\rho$  is the rubber mass density. Substitution of Eq. (2) into Eq. (1) yields

$$\sigma_f = \rho c_L V \int_{q_L}^{Q_c} q^3 C(q) P(q) dq. \quad (3)$$

The lower limit of integration is  $q_L = 2\pi/L$  with  $L$  the size of the nominal contact area ( $L \gg \xi$ ), and the upper limit of inte-

gration is  $Q_c = \pi/a_o$  with  $a_o$  of microscopic dimensions. Furthermore, if only elastic deformation occurs,  $P(q)$  is given by<sup>5</sup>

$$P(q) = \frac{2}{\pi} \int_0^{+\infty} \frac{\sin x}{x} e^{-x^2 G(q)} dx, \quad (4)$$

$$G(q) = \frac{\pi \rho^2 c_L^2 V^2}{2 \sigma_o^2} \int_{q_L}^q q^3 C(q) dq. \quad (5)$$

Although, at high sliding velocities the rubber is in the glassy region where  $c_L$  can be treated as constant (independent of frequency), for a real system wear and high local temperatures at the rubber/solid interface have to be taken also into account.

In the high velocity limit or  $\pi G(q) > 1$ , one should employ the expansion  $\sin x = \sum_{n=0, \infty} (-1)^n x^{2n+1} / (2n+1)!$  in Eq. (4), which yields

$$\mu_f = \frac{\sqrt{\pi\rho c_L}}{\sigma_o} \sum_{n=0}^{+\infty} \frac{(-1)^n}{(2n+1)2^{2n+1}n!} \left( \frac{\sigma_o^2}{\pi\rho^2 c_L^2} \right)^{n+1/2} V^{-2n} x$$

$$\times \int_{q_L}^{Q_c} q^3 C(q) dq \left\{ \frac{1}{2} \int_{q_L}^q q^3 C(q) dq \right\}^{-(n+1/2)}. \quad (6)$$

For very high velocity or  $\pi G(q) \gg 1$ , the first-order term of Eq. (6) yields

$$\mu_f = \int_{q_L}^{Q_c} q^3 C(q) \left[ \int_{q_L}^q q^3 C(q) dq \right]^{-1/2} dq. \quad (7)$$

Therefore, the coefficient of friction given by Eq. (7) is independent of the sliding velocity  $V$  (by neglecting also temperature effects and wear processes).<sup>5</sup> This is the result of the presence of the factor  $P(q)$  because otherwise the friction coefficient would grow linearly with the sliding velocity  $V$ . Moreover, Eq. (7) shows that the higher-order terms ( $n > 1$  in the expansion) decay as inverse power law ( $\sim V^{-2n}$ ) of the sliding velocity.

### III. RESULTS AND DISCUSSION

As Eqs. (4)–(7) indicate, in order to calculate the coefficient of friction  $\mu_f$  the knowledge of the roughness spectrum  $C(q)$  is necessary. A wide variety of surfaces/interfaces are well described by a kind of roughness associated with self-affine scaling,<sup>7</sup> for which  $C(q)$  scales as a power-law  $C(q) \propto q^{-2-2H}$  if  $q\xi \gg 1$ , and  $C(q) \propto \text{const}$  if  $q\xi \ll 1$  (Ref. 7). The roughness exponent  $H$  is a measure of the degree of surface irregularity,<sup>7</sup> such that small values of  $H$  characterize more jagged or irregular surfaces at short length scales ( $< \xi$ ). The self-affine scaling behavior is satisfied by the simple model<sup>8</sup>

$$C(q) = \frac{1}{2\pi} \frac{w^2 \xi^2}{(1 + a q^2 \xi^2)^{1+H}} \quad (8)$$

with  $a = (1/2H)[1 - (1 + a Q_c^2 \xi^2)^{-H}]$  if  $0 < H < 1$  (power-law roughness), and  $a = (1/2)\ln[1 + a Q_c^2 \xi^2]$  if  $H = 0$  (logarithmic roughness).<sup>8</sup> The parameter  $w$  is the rms roughness amplitude, and  $Q_c = \pi/a_o$  with  $a_o$  of the order of atomic dimensions. For other correlation models see also Refs. 9 and 10.

Substitution of Eq. (8) into Eq. (4) yields the analytic form

$$\int_{q_L}^q q^3 C(q) dq = \frac{1}{2\pi} \left[ \frac{w^2}{2a^2 \xi^2} \right] \left[ \frac{1}{1-H} \{T_q^{1-H} - T_L^{1-H}\} + \frac{1}{H} \{T_q^{-H} - T_L^{-H}\} \right] \quad (9)$$

with  $T_q = (1 + a q^2 \xi^2)$  and  $T_L = (1 + a q_L^2 \xi^2)$ . Equation (9) furthers the calculations of the friction coefficient  $\mu_f$ . For the limiting cases  $H=0$  and  $H=1$  one has to employ the identity  $\ln(x) = \lim_{c \rightarrow 0} (1/c)(x^c - 1)$ . Therefore, we obtain

$$\int_{q_L}^q q^3 C(q) dq|_{H=0} = \frac{1}{2\pi} \frac{w^2}{2a^2 \xi^2} \left[ a \xi^2 (q^2 - q_L^2) + \ln\left(\frac{T_L}{T_q}\right) \right], \quad (10)$$

$$\int_{q_L}^q q^3 C(q) dq|_{H=1} = \frac{1}{2\pi} \frac{w^2}{2a^2 \xi^2} \left[ \ln\left(\frac{T_q}{T_L}\right) + \{T_q^{-1} - T_L^{-1}\} \right]. \quad (11)$$

Moreover, since  $C(q) \propto w^2$ , Eq. (7) yields for the friction coefficient (at high velocities) the simple dependence  $\mu_f \propto w$ , while any complex dependence will arise solely from the roughness parameters  $H$  and  $\xi$ . If, however, we consider higher-order terms from Eq. (6), then the dependence on  $w$  is more complex. Indeed, the  $n$ -order term yields a contribution  $\sim w^{1-n}$ . If, however, we consider for the factor  $P(q)$  the interpolation form<sup>5</sup>  $P(q) = \{1 + [\pi G(q)]^{3/2}\}^{-1/3}$ , then the friction coefficient is given by the more complex expression

$$\mu_f = \frac{\sigma_f}{\sigma_o} = \frac{\rho c_L}{\sigma_o} V \int_{q_L}^{Q_c} q^3 C(q) \left[ 1 + V^3 \frac{\pi^3 \rho^3 c_L^3}{2\sigma_o^3} \left\{ \frac{1}{2} \int_{q_L}^q q^3 C(q) dq \right\}^{3/2} \right]^{-1/3} dq, \quad (12)$$

which indicates a more complex dependence on the roughness amplitude  $w$ .

Furthermore, as Fig. 2(a) indicates the friction coefficient  $\mu_f$  decreases with increasing correlation length  $\xi$  or decreasing roughness ratio  $w/\xi$  (for rms roughness amplitude  $w$  fixed) due to surface smoothing at large lateral roughness wavelengths. However, the relative decrement of the friction coefficient increases with increasing roughness exponent  $H$  or smoother surfaces at short wavelengths. Clearly the influence of the roughness exponent  $H$  on  $\mu_f$  is more significant at larger correlation lengths  $\xi$ .

Nonetheless, a peculiar behavior for the friction coefficient  $\mu_f$  develops for small roughness exponents  $H$  ( $< 0.3$ ) as Fig. 2(b) indicates. Indeed, for correlation lengths  $\xi < 200$  nm (or  $w/\xi > 0.01$ ) the friction coefficient  $\mu_f$  is lower in magnitude for smaller roughness exponents  $H$ , while the opposite behavior takes place for larger correlation lengths  $\xi$ . Moreover, the variation of the friction coefficient is faster for larger roughness exponents  $H$  in the small correlation length regime (or  $w/\xi > 0.05$ ).

If we examine the direct dependence of the friction coefficient  $\mu_f$  on the roughness exponent  $H$  then we also observe a nontrivial behavior. Clearly for rougher surfaces at large wavelengths or smaller correlation lengths  $\xi$ , the friction coefficient  $\mu_f$  has a maximum as a function of the roughness exponent  $H$  as Fig. 3(a) clearly indicates. The maximum position, however, shifts to lower roughness exponents  $H$  with increasing correlation length  $\xi$ . The magnitude of the maximum weakens drastically and disappears for very weak roughness (or  $w/\xi \ll 1$ ) as Fig. 3(b) indicates. Moreover, the presence of a maximum at moderate correlation lengths  $\xi$  indicates a multivalued behavior of  $\mu_f$  with respect to the roughness exponent  $H$ .

If we reduce further the correlation length  $\xi$ , the friction coefficient  $\mu_f$  increases with increasing roughness exponent  $H$  [Fig. 4(a)]. The latter appears rather contrainuitive, as it points against the notion that the rougher the surface the

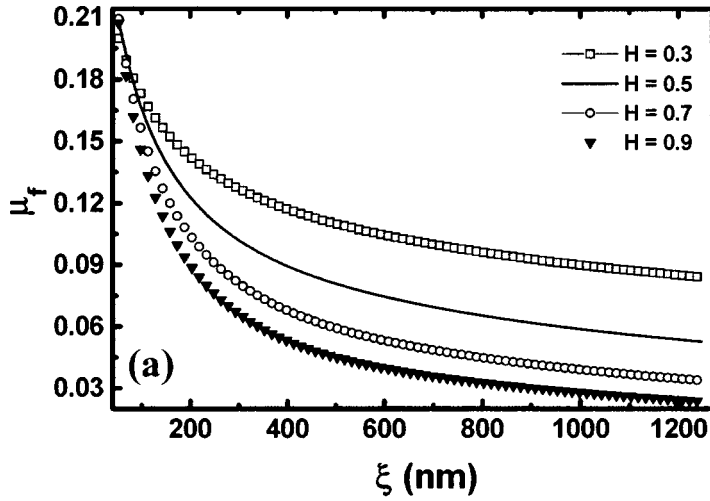
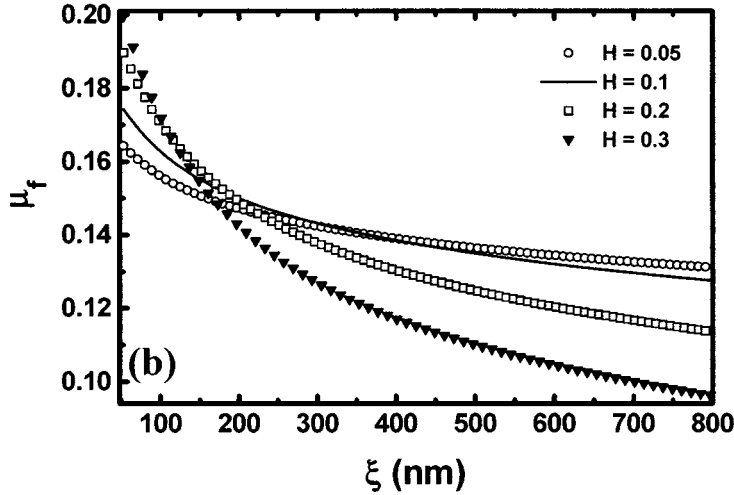


FIG. 2. (a) Friction coefficient  $\mu_f$  vs roughness correlation length  $\xi$  with  $w=5$  nm,  $a_o=0.3$  nm,  $L=100$   $\mu$ m, and various roughness exponents  $H (\geq 0.3)$ . (b) Same as in (a) but for low roughness exponents  $H (\leq 0.3)$ .



higher the friction coefficient. The latter is shown in Figs. 2 and 3 after the position of the maximum. However, the presence of the maximum, in Fig. 3(a) and the continuous increment of the friction coefficient  $\mu_f$  for small correlation lengths  $\xi$  as in Fig. 4(a) are taking place within the strong roughness limit  $|\nabla h| > 1$ . The latter is well quantified in terms of the local surface slope  $\rho_{rms} = \sqrt{\langle |\nabla h|^2 \rangle}$  or

$$\rho_{rms} = \sqrt{(2\pi) \int_{q_L}^{Q_c} q^3 C(q) dq} = \left[ \frac{w}{\sqrt{2}a\xi} \right] \left[ \frac{1}{1-H} \{T_{Q_c}^{1-H} - T_L^{1-H}\} + \frac{1}{H} \{T_{Q_c}^{-H} - T_L^{-H}\} \right]^{1/2}, \quad (13)$$

which as Fig. 4(b) indicates is rather large ( $\rho_{rms} > 1$ ; strong roughness) for small correlation lengths  $\xi$  and small roughness exponents ( $H < 0.5$ ). The latter is responsible for the behavior shown in Figs. 4(a) and 3. Therefore, in the limit of strong roughness ( $\rho_{rms} > 1$ ) as a function of the lateral corre-

lation length  $\xi$ , there is a limiting value of  $\xi_o$  below that the friction coefficient  $\mu_f$  increases with increasing roughness exponent  $H$ . At any rate, this is the result of the presence of the contact factor  $P(q)$  in Eq. (3) that effectively yields the friction coefficient  $\mu_f$ . If the contact factor  $P(q)$  is set equal to unity then not only  $\mu_f$  would increase with increasing sliding velocity  $V$ , but also would follow the behavior of the average local slope  $\rho_{rms}$  with respect to the self-affine roughness parameters  $w$ ,  $\xi$ , and  $H$  [Fig. 4(b)].

Finally, we should point out that in actual situations besides adhesive and hysteric friction, the rubber produces traction forces through tearing and wear. As deformation stresses and sliding speeds increase (e.g., tires in racing cars), the local stress can exceed the tensile strength of the rubber especially near the point of a sharp irregularity. The high local stress can deform the internal rubber structure beyond the point of elastic recovery. Indeed, when polymer bonds and cross-links are stressed to failure the material can no longer recover completely, leading to tearing. The latter absorbs

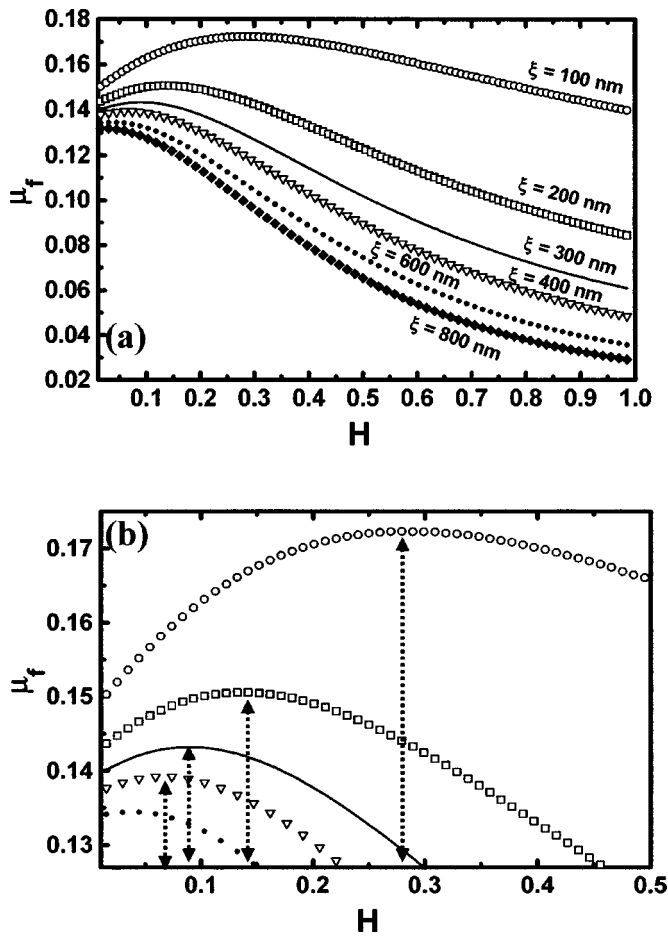


FIG. 3. (a) Friction coefficient  $\mu_f$  vs roughness exponent  $H$  with  $w=5$  nm,  $a_o=0.3$  nm,  $L=100$   $\mu$ m, and various roughness correlation lengths  $\xi$ . (b) Friction coefficient  $\mu_f$  vs roughness exponent  $H$  with the same parameters as in Fig. 3(a), but with greater detail around the maximum.

energy and results in additional friction forces within the contact surface. Wear processes is the ultimate result of tearing.

#### IV. CONCLUSIONS

In summary, the coefficient of kinetic friction  $\mu_f$  at high sliding velocities of rubbers onto solid substrates can be strongly influenced by the roughness characteristics (in the absence of wear and local heating processes). It is shown that the friction coefficient decreases with increasing correlation length  $\xi$  and increasing roughness exponent  $H$  for significantly large correlation lengths. For sufficiently small correlation lengths the opposite behavior takes place since the system is within the strong roughness limit or equivalently local surface slopes larger than 1. The complexity of the situation is revealed in direct plots of the friction coefficient as a function of the roughness exponent  $H$ . For large correlation lengths the friction coefficient decreases with increasing  $H$ . However, as the correlation length  $\xi$  decreases, a maximum occurs followed by a continuous decrement of the friction coefficient with decreasing  $H$  and  $\xi$ .

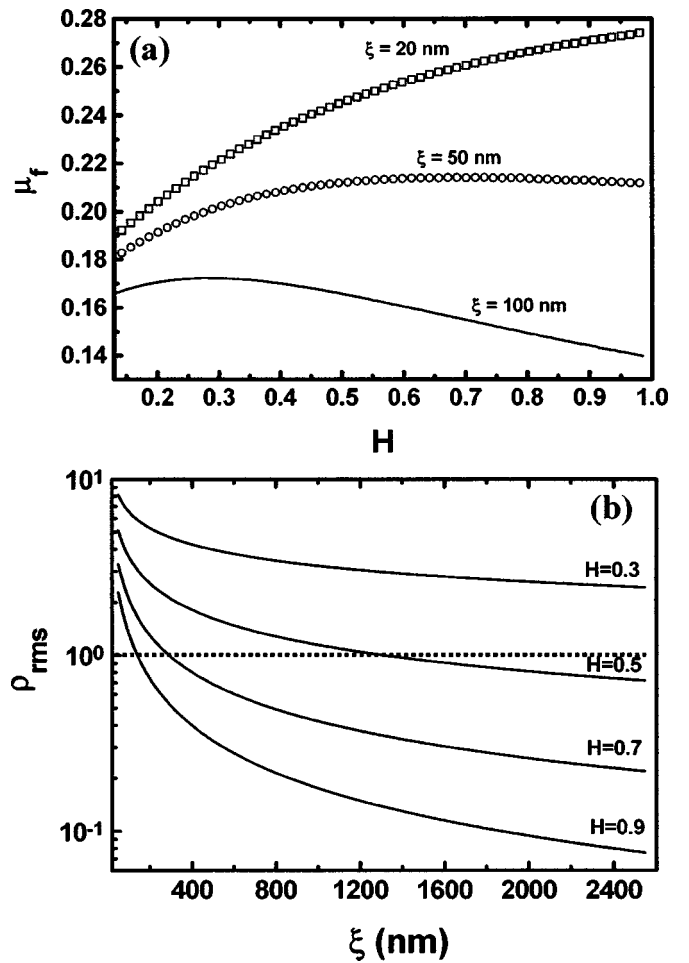


FIG. 4. (a) Friction coefficient  $\mu_f$  vs roughness exponent  $H$  with  $w=5$  nm,  $a_o=0.3$  nm,  $L=100$   $\mu$ m, and various relatively low roughness correlation lengths  $\xi$ . (b) Local surface slope  $\rho_{rms}$  vs the roughness correlation length  $\xi$  for various roughness exponents  $H$ . The dotted line indicates the weak roughness regime ( $\rho_{rms} < 1$ ).

#### ACKNOWLEDGMENTS

I would like to acknowledge useful discussions with G. Backx and J. Th. M. DeHosson for contact related problems on rough surfaces.

#### APPENDIX

In the more general case of lower sliding velocities one must use Eq. (1) for  $M_{zz}$ , the more general expression of which Eq. (2) is a limiting case.<sup>5</sup> In this case, if we define  $S = (\omega^2 c_T^{-2} - 2q^2)^2 + 4q^2 P \tilde{P}$  with  $\tilde{P} = \pm (\omega^2 c_T^{-2} - q^2 \pm j\varepsilon)^{1/2}$ ,  $P = \pm (\omega^2 c_L^{-2} - q^2 \pm j\varepsilon)^{1/2}$ , (where  $\varepsilon$  is an infinitesimal positive number and  $\pm$  corresponds, respectively, to positive and negative frequencies  $\omega$ ), transverse and longitudinal sound velocities, respectively, by  $c_T^2 = E[2\rho(1+\nu)]^{-1}$  and  $c_L^2 = E(1-\nu)[\rho(1-2\nu)(1+\nu)]^{-1}$ , the tensor  $M_{zz}$  along the  $z$  direction is given by<sup>5</sup>

$$M_{zz} = -j \frac{1}{\rho c T^2} \frac{P(q, \omega)}{S(q, \omega)} \left( \frac{\omega}{c_T} \right)^2 \quad (\text{A1})$$

with the elastic modulus  $E$  and Poisson ratio  $\nu$  depending on frequency. A qualitative model for the elastic modulus  $E(\omega)$  is given by the rheological model<sup>5</sup>

$$E(\omega) = \frac{E_1[(1 + \alpha) + (\omega\tau)^2]}{(1 + \alpha)^2 + (\omega\tau)^2} - j \frac{\alpha\omega\tau E_1}{(1 + \alpha)^2 + (\omega\tau)^2} \quad (\text{A2})$$

with  $E_1 = E(\infty)$ ,  $E(\infty)/E(0) = 1 + \alpha$  (typically  $\alpha = 10^3$ ), and  $1/\tau$  the flip rate of molecular segments, which are configuration changes responsible for the viscoelastic properties of the rubber body.

---

\*Email address: G.palasantzas@phys.rug.nl

<sup>1</sup>D. F. Moore, *The Friction and Lubrication of Elastomer* (Pergamon, Oxford, 1972); M. Barguis, *Mater. Sci. Eng.* **73**, 45 (1985); A. D. Roberts, *Rubber Chem. Technol.* **65**, 673 (1992).

<sup>2</sup>K. A. Grosch, *Proc. R. Soc. London, Ser. A* **274**, 21 (1963).

<sup>3</sup>J. A. Greenwood, *Fundamentals of Friction, Macroscopic and Microscopic Processes*, edited by I. L. Singer and H. M. Polack (Kluwer, Dordrecht, 1992); J. A. Greenwood and J. B. P. Williamson, *Proc. R. Soc. London, Ser. A* **295**, 300 (1966).

<sup>4</sup>B. N. J. Persson, *Sliding Friction: Physical Principles and Applications*, 2nd ed. (Springer, Heidelberg, 2000).

<sup>5</sup>B. N. J. Persson, *J. Chem. Phys.* **115**, 3840 (2001). Besides the treatment of self-affine rough surfaces, for other friction studies on fractal rough surfaces, see also A. Majumdar and B. Bhushan, *J. Tribol.* **113**, 1 (1991).

<sup>6</sup>B. B. Mandelbrot, *The Fractal Geometry of Nature* (Freeman,

San Francisco, 1982).

<sup>7</sup>J. Krim and G. Palasantzas, *Int. J. Mod. Phys. B* **9**, 599 (1995); Y.-P. Zhao, G.-C. Wang, and T.-M. Lu, *Characterization of Amorphous and Crystalline Rough Surfaces—Principles and Applications*, *Experimental Methods in Physical Science*, Vol. 37 (Academic Press, New York, 2001); P. Meakin, *Fractals, Scaling, and Growth Far from Equilibrium* (Cambridge University Press, Cambridge, England, 1998).

<sup>8</sup>G. Palasantzas, *Phys. Rev. B* **48**, 14 472 (1993); **49**, 5785(E) (1994).

<sup>9</sup>S. K. Sinha, E. B. Sirota, S. Garoff, and H. B. Stanley, *Phys. Rev. B* **38**, 2297 (1988); H.-N. Yang and T.-M. Lu, *Phys. Rev. E* **51**, 2479 (1995); Y.-P. Zhao, G.-C. Wang, and T.-M. Lu, *Phys. Rev. B* **55**, 13 938 (1997); G. Palasantzas and J. Krim, *Phys. Rev. B* **48**, 2873 (1993).

<sup>10</sup>G. Palasantzas, *Phys. Rev. E* **49**, 1740 (1994).